Journal of Applied Polymer Science

Biocomposite proton-exchange membrane electrolytes for direct methanol fuel cells

S Suganthi, S Mohanapriya, V. Raj
Advanced Materials Research Laboratory, Department of Chemistry, Periyar University, Salem 636011, India
Correspondence to: V. Raj (E-mail: doctorvraaj@gmail.com)

ABSTRACT: Poly(vinyl alcohol) (PVA)-amino acid (AA) biocomposite membranes are prepared by blending PVA with AAs such as glycine, lysine (LY), and phenyl alanine followed by *in situ* crosslinking with citric acid (CA) and explored as a new class of biocomposite membrane electrolytes for direct methanol fuel cells (DMFCs). CA crosslinks with PVA through esterification offers adequate chemical, thermal, and morphological stability thereby produces methanol-obstructing close-packed polymeric network. These biocomposite membranes are characterized in terms of mechanical, thermal, sorption, and proton-conducting properties. Hydrophilic nature of AA zwitterions significantly facilitates proton conduction and CA crosslinking mitigates methanol crossover through establishing appropriate balance between hydrophilic/hydrophobic domains. The rational design of membrane microstructure with proper arrangement of hydrophobic/hydrophilic domains is a key to enhance electrochemical selectivity of PVA-AA/CA biocomposite membranes. Biocomposite membrane comprising LY exhibits nearly threefold higher electrochemical selectivity in relation to PVA/CA blend membrane. © 2016 Wiley Periodicals, Inc. J. Appl. Polym. Sci. **2016**, *133*, 43514.

KEYWORDS: applications; biomaterials; composites; membranes

Received 30 November 2015; accepted 4 February 2016
DOI: 10.1002/app.43514

INTRODUCTION

Direct methanol fuel cells (DMFCs) represent a class of polymer electrolyte membrane (PEM) fuel cells (PEFCs), appropriate for portable devices or transportation applications in the view of their advantages such as high energy density, easy manipulation, and high efficiency.[1–4] PEM is an integral component of a fuel cell, which effectively separates the electrodes and facilitates proton conduction; thus, PEM completes the electrical circuit in the fuel cell. A typical PEM should have chemical, thermal, and morphological stability. Additionally, to act as a good DMFC electrolyte, it should possess superior methanol-barrier characteristics. Commonly used electrolyte for DMFC is Nafion, the only advanced perfluroinated ionomeric membrane with high proton conductivity, good mechanical strength along with high thermal and chemical stability. The wide-spread applications of DMFC is however hampered due to phenomenon of methanol crossover that arises due to the passage of methanol from anode to cathode through PEM during DMFC operation.[5,6] This redundant methanol crossover phenomenon accounts for the depolarization and conversion losses. It is estimated that about 40% of methanol could be wasted by the penetration of methanol across Nafion electrolyte membrane.[7–10] The critical drawback primarily associated with Nafion is high methanol permeability ($\sim 10^{-6}$ cm^2/s), which severely reduces the DMFC performance. Also cost of Nafion is high.[11–14] In the light of the foregoing, intensive research efforts are being expended towards modification of fluorinated and nonfluorinated membranes to minimize methanol crossover across DMFC electrolyte.[15–18] Hence, through rationally designing and screening the appropriate materials, it is quite feasible to obtain composite DMFC membranes with a low methanol crossover and high proton conductivity.

Poly(vinyl alcohol) (PVA)-based membranes are used as DMFC electrolytes because (i) they preferentially permeate water (ii) possess good mechanical and chemical stability (iii) are cost-effective.[19] PVA is a hydrophilic, semicrystalline, nontoxic, and cost-effective biodegradable polymer. However, PVA in its pristine form possess poor conductivity and mechanical properties. To improve proton conductivity and methanol permeability characteristics, it is modified with the addition of different polymers, inorganic fillers, metal oxide nanoparticles, etc.[20–24]

Accordingly, present study is an attempt to modify PVA with biomolecules namely amino acids (AAs), with a view to enhance proton conductivity and reduce the methanol crossover. It is well-known that AA consists of both carboxylic acid (–COOH) and amino ($-NH_2$) groups placed within the same molecule, could acts as both a proton donor and a proton acceptor. AA exists as a zwitter ion which successfully transmits

the protons through intra and intermolecular proton exchange. Hydroxyl groups (-OH) of PVA effectively interact with functional groups of AA which results in improved hydrophilicity and thermo-mechanical properties.[25,26]

It is established that crosslinking conditions such as nature of crosslinker, amount of crosslinking agent, duration, and temperature of crosslinking reaction together play a decisive role in determining the membrane properties.[27] Several reports showed that chemical crosslinking of PVA with the orthophosphoric acid (H_3PO_4), hypophosphorus acid (H_3PO_2), sulfuric acid, glutaraldehyde, maleic unhydride, and sulfosuccinic acid could primarily influence methanol crossover and conductivity properties.[28–31] Rhim *et al.*[32] established dependence of proton conductivity and methanol permeability as a function of crosslinking temperature and amount of crosslinking agent using sulfosuccinic acid as a crosslinker. It is well documented in the literature that proton conduction occurs through the ionic channels assembled by hydrobhobic and hydrophilic domains and phase separated by micro or nanoscale. Methanol permeation happens mainly through these ionic channels; consequently, it depends on the dimension of these channels. Therefore, to mitigate the methanol crossover, it is essential to reduce the size of the ionic channels without disrupting proton-conducting path. This could be achieved by organizing adequate microdomains through appropriate crosslinking. Thus, suitable crosslinker is necessary to obtain a balance between hydrophobic and hydrophilic microstructure, which frames highly proton-conducting methanol-impermeable network. In this context, to fine-tune the properties of PVA, citric acid (CA) is used as a crosslinker, which establishes proper proportion between hydrophilic and hydrophobic domains. CA is a cheap, nontoxic polycarboxylic acid and has been used to improve the performance properties of cellulose, proteins, and so forth, in textile applications.[33] CA comprises both carboxylic acid and hydroxyl groups, hence could effectively involve in hydrogen bonding and crosslink with PVA through esterification reaction thereby ascertain proper arrangement of micro domains within PVA. It is illustrious that suitable proportion of hydrophilic/hydrophobic domain is essential to create proton conducting channels, prevent the methanol passage, and maintain good thermo-mechanical properties. Our research is aimed to improve the transport ability of PVA, through CA crosslinking. Crosslinking introduces reactive carboxylic acid groups in the PVA matrix and is expected to increase the active sites on the surface of PVA membrane, through which ions could be transported via hydrogen bonds. The ability of hydrophilic group to interact with water molecules and the hydrophobic group to be connected the surface of the material will reduce the surface tension arising from the contact of a solid material with a solution therefore impose mechanical stability.[34]

Eventually, the purpose of this investigation is to understand the transport behavior, such as proton conductivity and methanol permeability of PVA-AA biocomposite membrane crosslinked with CA (PVA-AA/CA). AAs render the PVA matrix hydrophilic whilst CA crosslinking provides hydrophobic backbone with ample stability. The functional groups belong to AA and CA could actively participate in hydrogen bonding therefore enhancing the thermo-mechanical stability and proton conductivity of the polymer. Hence, both proton conductivity and methanol permeability of PVA could be fine-tuned by blending it with AA followed by *in situ* crosslinking with CA. To the best of our knowledge, no literature is available on PVA-AA/CA biocomposite membrane electrolytes used for DMFC applications. The study proves that modification of PVA with AA followed by CA crosslinking can have an incredible impact on the hydrophilic/hydrophobic domain microstructure.

EXPERIMENTAL

PVA (99.7% hydrolyzed, M.W. 115,000) was obtained from Loba Chemie, India. Glycine (GL), lysine (LY), and phenyl alanine (PA) were procured from Acros organics. CA was obtained from SRL chemicals. Sulfuric acid (98%) was obtained from S.D. Fine Chemicals, India. All the chemicals were used as-received. Deionized (DI) water (18.4 MΩ cm) from Millipore was used during the experiments.

Membrane Preparation

PVA-AA biocomposite membranes were prepared by solution-casting technique. In brief, 30 mL of 4 wt % PVA solution was prepared by dissolving the required amount of PVA in water at 333 K followed by mechanical stirring until a clear solution was obtained. Similarly, 20 mL of 10 wt % AA in relation to PVA was dissolved in aqueous medium at 303 K followed by stirring until a homogeneous solution was obtained. Both the solutions were mixed and further stirred for 2 h to form a compatible blend. The composition of AAs was varied from 5 to 20 wt % in relation to PVA and optimized to 10 wt % with respect to mechanical stability. About 10 wt % of CA in relation to PVA was added as a crosslinker followed by the addition of a drop of sulfuric acid to catalyze the reaction. The mixture was allowed to stir at 333 K for 1 h to complete the crosslinking reaction. The viscous solution was cast on a flat Plexiglass plate to form a membrane by evaporating the solvent at room temperature (~303 K). PVA blend membrane was prepared in a similar manner without the addition of AAs. After evaporation of solvent, the membranes were dried at room temperature and the thickness of the membranes was ~160 μm. It is notable that when the AA content was above 10 wt %, in relation to polymeric matrix, membrane brittleness increased.

Ion-Exchange Capacity

Ion-exchange capacity (IEC) specifies the number of milli-equivalent of ions in 1 g of the membrane. To estimate IEC, membranes of similar weights were soaked in 50 mL of 0.01N sodium hydroxide solutions for 12 h at room temperature (303 K) and 10 mL of the solution was titrated against 0.01*N* sulfuric acid. The sample was regenerated with 1N hydrochloric acid, washed copiously with water to remove acid and dried to a constant weight. IEC was estimated from eq. (1) given below.

$$\mathrm{IEC} = \frac{(B-P)\times 0.01\times 5}{m} \quad (1)$$

In eq. (1), IEC is the ion exchange capacity (in meq/g), B is the amount of sulfuric acid used to neutralize blank sample solution (mL), P is the amount of H_2SO_4 used to neutralize the biocomposite membrane-soaked solution (mL), 0.01 is the

normality of H_2SO_4, 5 is the factor corresponding to the ratio of the amount of NaOH used to soak the membrane to the amount used for titration, and m is membrane mass (g).

Sorption and Proton Conductivity Measurements

For sorption measurements, circularly cut (diameter = 2.5 cm) PVA blend and PVA-AA/CA biocomposite membranes were dipped in deionized water for 24 h to attain equilibrium. The membranes were surface blotted and initial mass values were recorded on a single-pan digital microbalance (Sartorius, Germany) within an accuracy of ±0.01 mg. The membranes were then dried in a vacuum oven at 373 K for 24 h and their respective weights were measured. Sorption values for aforesaid membranes were calculated using eq. (2) given below.

$$\%\ \text{Sorption} = \left(\frac{W_\infty - W_\circ}{W_\circ}\right) \times 100 \tag{2}$$

In eq. (2), W_∞ and W_o refer to the weights of sorbed and dry membranes, respectively.

Proton conductivity measurements were performed on PVA blend and PVA-AA/CA biocomposite membranes in a two-probe cell by AC impedance technique. The conductivity cell comprised two stainless-steel electrodes, each of 20 mm diameters. The membrane sample was sandwiched between these two electrodes mounted in a Teflon block and kept in a closed glass container. The ionic conductivity data for the membranes were obtained under fully humidified condition (100%) by keeping deionized water at the bottom of the test container and equilibrating it for ~24 h. Subsequently, conductivity measurements were conducted between 303 and 373 K in a glass container with the provision to heat. The temperature was constantly monitored with a thermometer kept inside the container adjacent to the membrane. AC impedance spectra of the membranes were recorded in the frequency range between 1 MHz and 10 Hz with 10-mV amplitude using potentiostat. The resistance (R) of the membrane was determined from the high-frequency intercept of the impedance with the real axis and the membrane conductivity was calculated from the membrane resistance, R, from:

$$\sigma = \left(\frac{l}{R \times A}\right) \tag{3}$$

In eq. (3), σ is the proton conductivity of the membrane (S/cm), l is the membrane thickness (cm), and A is the membrane cross-sectional area (cm^2).

Physicochemical Characterization

Universal testing machine (UTM) (Model AGS-J, Shimadzu) with an operating head-load of 10 kN was used to study the mechanical properties of the membranes. Cross-sectional area of the sample was obtained from the initial width and thickness of the membrane sample. The test samples were prepared in the form of dumb-bell shaped object as per ASTM D-882 standards. The membranes were then placed in the sample holder of the machine. The film was stretched at a cross-head speed of 1 mm/min and its tensile strength was estimated using eq. (4).

$$\text{Tensile strength} = \frac{\text{Maximum load}}{\text{Cross-sectional area}} \tag{4}$$

Surface micrographs for PVA blend membrane and PVA-AA/CA biocomposite membranes were obtained using JEOL JSM 35CF scanning electron microscope (SEM). Gold film of thickness <100 nm was sputtered on the membrane surfaces using a JEOL Fine Coat Ion Sputter-JFC-1100 Unit, before their examination under SEM. Thermo-gravimetric analysis of all the membranes were carried out using an SDT Q600 V8.2 TGA/DTA instrument in the temperature range between 273 and 1073 K at a heating rate of 5 K/min with nitrogen flushed at 200 mL/min. The FTIR spectra for PVA blend and PVA-AA/CA biocomposite membranes were obtained using a Nicolet IR 860 spectrometer (Thermo Nicolet Nexus-670) in the frequency range between 4000 and 400 cm^{-1}.

Methanol-Permeation Studies

Methanol permeability of these membranes was determined by a procedure mentioned elsewhere using gas chromatography.[35] In brief, permeability is determined by clamping the membrane in a glass cell between two chambers each approximately holds 50-mL solution. One compartment of the cell was filled with 2M methanol solution and the other with deionized water. The membrane (effective area 2.5 cm^2) was clamped between the two compartments which were kept under stirring during experiment. The methanol concentration in the receptor chamber was measured with respect to time using a gas chromatography (Shimazu GC-14B) equipped with a thermal conductivity detector. The methanol permeability was calculated by the following equation:

$$P = \left(\frac{V_B \times l}{A \times C_{AO}}\right) \times S \tag{5}$$

where S is the slope of the straight line of concentration versus time plot, V_B is the volume of the receptor compartment, and l, A, and C_{A0} were the membrane thickness, effective membrane area, and feed concentration, respectively. Before testing, membranes were hydrated in deionized water for at least 24 h.

RESULTS AND DISCUSSION

Water Sorption and IEC Studies' of Membranes

In accordance with IEC data as indicated in Table I, concentration of ion-exchangeable groups has increased upon the addition of AA into PVA. Since IEC of a membrane relies on number of ion-exchange groups, it is deduced that amino and carboxylic acid groups of AA have improved mobility of exchanged ions within the polymeric blend resulting in higher IEC. In addition to this, hydroxyl and carboxylic groups present in CA contribute to the enhancement of IEC. As IEC provides a reliable approximation about proton conductivity, it is reasonable to believe that AAs could raise the proton conductivity. It is noteworthy that marginal variation in IEC values of biocomposites is observed, which suggests that the conductivity depends on the nature of AA.

It is well known that the swelling properties have a huge influence on both stability and proton conductivity of a PEM.[36–38] Optimal water uptake is desirable for a membrane because higher water sorption facilitates proton conduction while

Table I. Sorption Characteristics and IEC Values of PVA/CA Blend and PVA-AA/CA Biocomposite Membranes

Type of membrane[a]	% Water sorption	% Methanol sorption	IEC (meq/g)
PVA/CA blend	42.5	27.1	0.52
PVA-GL/CA biocomposite	61.8	25.3	0.62
PVA-PA/CA biocomposite	65.8	24.2	0.7
PVA-LY/CA biocomposite	64.6	24.1	0.79

[a] Triplicate measurements were carried out to confirm the values and standard error is about ± 3%.

adversely affects the dimensional stability. The effect of AA addition into PVA, toward the water and methanol uptake of the fabricated biocomposite membrane is presented in Table I. Water and methanol sorption depends on the extent of crosslinking and hydrophilic groups in the prepared structure. Water uptake associated with both PVA blend and PVA-AA/CA biocomposite membranes is higher compared to methanol uptake. This is attributed to the higher affinity of membranes towards water molecules. The hydrophilic amino and carboxylic acid groups present in AA helps to absorb more water. On the other hand, the incorporation of AA into PVA increased the water uptake while decreasing methanol uptake of PVA-AA/CA biocomposite membranes. This result suggests that PVA-AA/CA biocomposites have priority to absorb water molecules therefore suppress the methanol transport through them. The order of water uptake of membranes is PVA-LY/CA> PVA-PA/CA> PVA-GL/CA> PVA. From these results, it follows that carboxylic acid and amino groups essentially increase water retaining capability of biocomposite membranes. It is well known that the water molecules, which reside in the hydrophilic domains of polymeric structure, facilitate proton transportations. However, too much water absorption could result in the loss of mechanical stability. In this regard, the crosslinking of PVA with CA not only enhances the mechanical properties of the membranes, but also the presence of functional groups belong to CA provides space for more accommodation of H_2O molecules. Besides, the interactions between PVA-AA and CA such as ionic crosslinking (electrostatic forces) and hydrogen-bonding bridges, contribute to the control of membrane swelling without a decrease in flexibility. These hydrogen bonds offer well-connected path for the transmission of protons by bringing the proton-conducting groups closer. Accordingly, hydrophilic nature of the biocomposites shows more affinity toward water which in turn may impact membrane properties. Improved water uptake promotes the proton transport due to the decrease in distance between ionic groups of PVA and AA. The effect of the enhanced proton conduction of the composite membranes was evaluated by the conductivity measurements. From the sorption studies, it is to be predicted that the PVA-AA/CA biocomposite membranes will have excellent methanol-barrier characteristics along with good thermo-mechanical stability and high mechanical flexibility. These features are prime requirements of a membrane to perform as a DMFC electrolyte.

UV And FTIR Spectral Analyses

Analysis of UV spectra of pure PVA, LY, and PVA-LY provide evidence for the successful blending of polymer with AA and the results are provided in Figure 1. The spectra of pure PVA exhibited a shoulder-like band at 250 nm, whereas it lies at 195 nm in case of pure LY. On blending the PVA with LY, it is observed that absorption peak of PVA shifts toward a lower wavelength. From these results, it is clear that functional groups

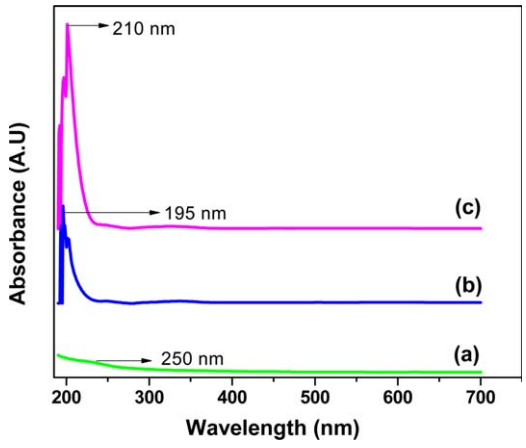

Figure 1. UV–visible absorption spectra: (a) PVA blend (b) LY and (c) PVA-LY solutions. [Color figure can be viewed in the online issue, which is available at wileyonlinelibrary.com.]

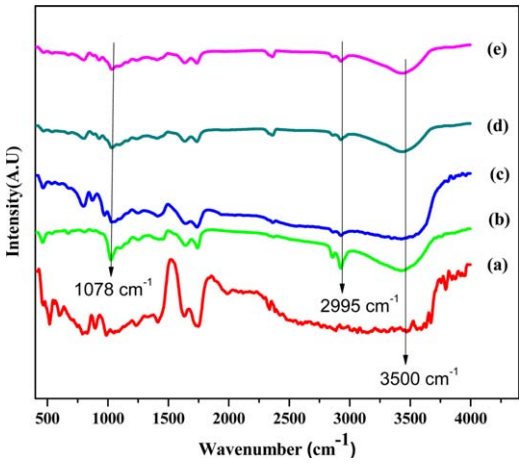

Figure 2. FTIR spectra of (a) PVA crosslinked with CA, (b) noncrosslinked PVA, (c) PVA-LY/CA, (d) PVA-GL/CA, and (e) PVA-PA/CA membranes. [Color figure can be viewed in the online issue, which is available at wileyonlinelibrary.com.]

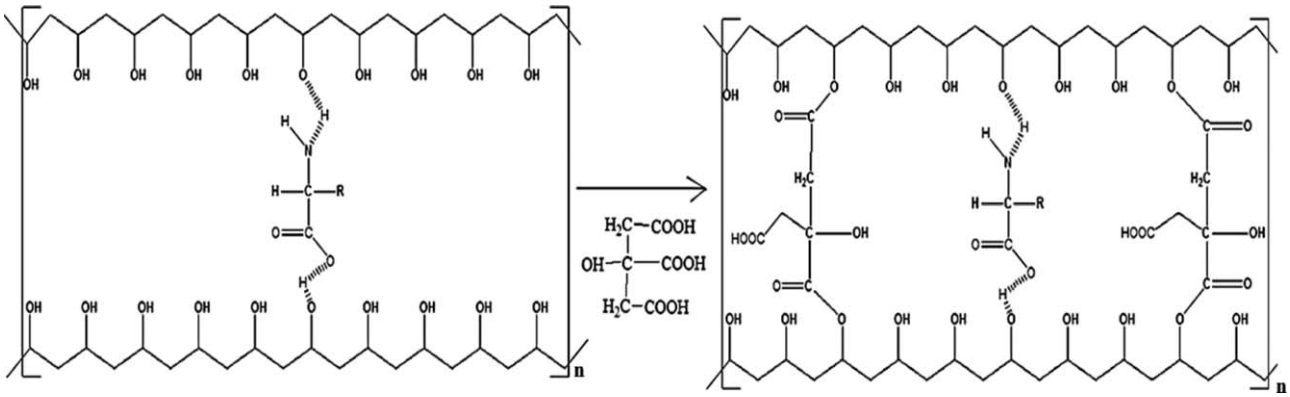

Scheme 1. Crosslinking reaction between PVA/AA polymer chains and Citric acid.

belong to LY interacts strongly with hydroxyl groups of PVA through hydrogen bonding.

Crosslinking of PVA chains with CA has been followed through recording FTIR spectra of noncrosslinked and crosslinked PVA. Also, blending of PVA with AA is elucidated by evaluating the FTIR spectra of PVA-AA and the results are presented in Figure 2. Intramolecular and intermolecular hydrogen bonds are expected to occur among PVA chains due to high hydrophilic forces. A broad band centered at 3500 cm^{-1} relates to intermolecular hydrogen bonding and -OH stretching vibration of PVA as shown in pure PVA spectra [Figure 4(a)]. Characteristic absorption of semicrystalline PVA occurred at 1142 cm^{-1}.[39] An absorption band at 1110 cm^{-1} can be attributed to the vibration of C-O groups of PVA. A distinct absorption band at 1078 cm^{-1}, appeared in PVA/CA spectra might be ascribed to C-O ester groups, indicating the crosslinking reaction through esterification between CA and PVA chains, as seen from Figure 2(b). Also, it could be noticed from the spectrum of CA crosslinked PVA [Figure 2(b)] that O-H stretching vibration peak (3330–3350 cm^{-1}) is decreased when compared to that of pure PVA [Figure 2(a)]. This result suggests that the hydrogen bonding becomes weaker in crosslinked PVA than in pure PVA because of decrease in the number of -OH groups. In addition, the C-O stretching at approximately 1100 cm^{-1} in FTIR spectrum of pure PVA is replaced by a broader absorption band (from 1000 to 1140 cm^{-1}), which can be attributed to the ester (C-O) bands formed by the crosslinking reaction of PVA with CA, as shown in reaction (Scheme 1).

Positions of the vibration modes of PVA/CA and AA are merged together as represented by the spectrum of PVA-AA/CA spectra [Figure 2(c–e)]. Hence spectral features of PVA-AA/CA illustrate combination of both PVA/CA and AA with few peaks appearing newly and other peaks appeared accompanied with a shift in their position. Spectral properties of PVA/CA are strongly influenced by the interaction of AA with the polymer backbone. Distinct absorption of AA due to presence of amino and carboxylic groups occurred in all PVA-AA/CA biocomposites indicating successful blending of PVA with AA. Spectral characteristics of PVA-AA are modified depending on the nature of AA. A broad band from 2600 to 3400 cm^{-1} centered at around 3000 cm^{-1} present in all the spectra of PVA-AA/CA is generally assigned to NH_3^+ stretching of AA.[40] Both symmetric and asymmetric vibrations of amino groups appear at around 1550 and 1650 cm^{-1}, respectively.[41] In modified samples, these peaks overlap with broad bands of the stretching and deformation modes of carboxylic and amino groups of AA as evident from the spectra.

Thermo-Mechanical Stabilities of Membranes

TGA data for PVA blend and PVA-AA/CA biocomposite membranes are shown in Figure 3. Three main degradation stages occur due to the processes of thermal solvation, thermal degradation, and thermal oxidation of the polymeric matrices as reported for similar kind of membranes.[42] Comparison of the TGA curves of the membranes reveals that the degradation trends of PVA/CA blend and PVA-AA/CA biocomposite membranes are almost the same. Also, thermal stability of PVA/CA is hardly affected due to blending with AA however, additional hydrogen bonds formed through CA crosslinking provides sufficient thermal stability. It is clear from the thermal studies that biocomposite membranes are thermally stable under

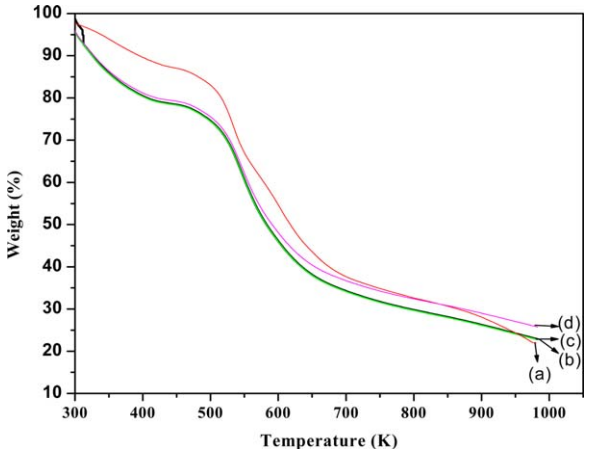

Figure 3. TGA plots for (a) PVA/CA blend membrane, (b) PVA-GL/CA, (c) PVA-PA/CA, and (d) PVA-LY/CA biocomposite membranes. [Color figure can be viewed in the online issue, which is available at wileyonlinelibrary.com.]

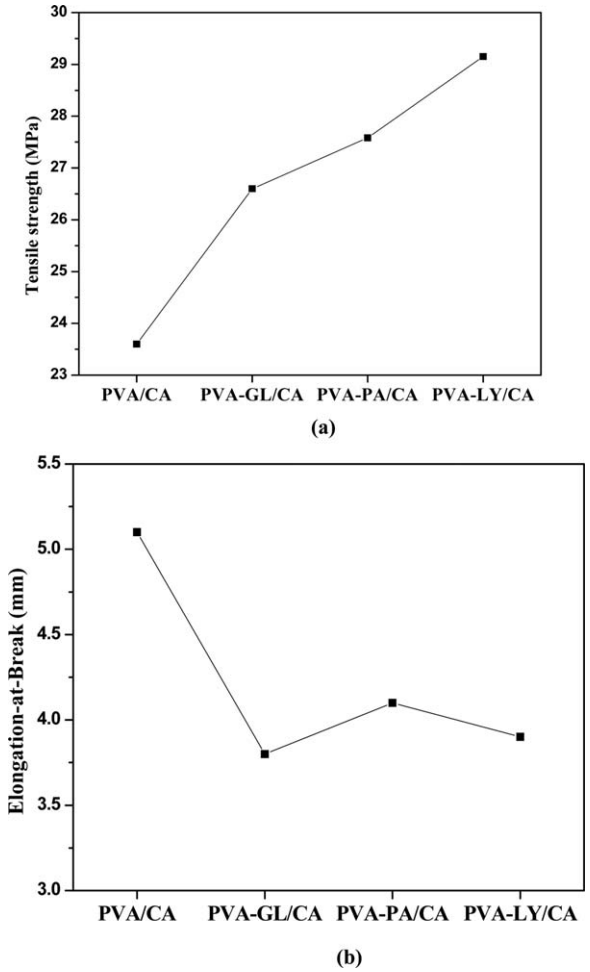

Figure 4. (a) Tensile strength of PVA blend, PVA-GL PVA-GL/CA, PVA-PA/CA, and PVA-LY/CA biocomposite membranes. (b) Elongation-at-break determined for PVA blend, PVA-GL/CA PVA-GL/CA, PVA-PA/CA, and PVA-LY/CA biocomposite membranes.

DMFC operating conditions because onset of thermal degradation of all PVA-AA/CA biocomposite membranes begins at 473 K.

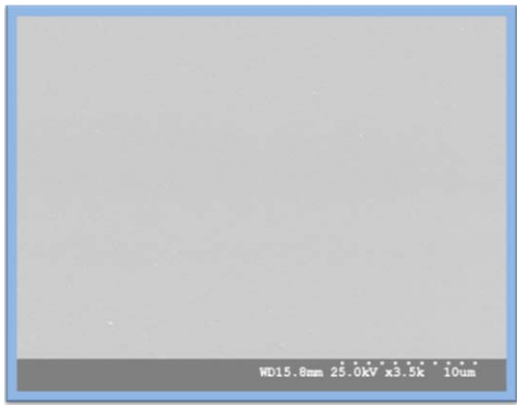

Figure 5. Scanning electron micrograph of PVA-LY/CA biocomposite membrane. [Color figure can be viewed in the online issue, which is available at wileyonlinelibrary.com.]

The mechanical properties of all the membranes were determined by its tensile strength and elongation-at-break as presented in Figure 4. It is evident from the data that blending AA only marginally improved the tensile strength and resulting PVA-AA/CA biocomposite membranes possess good stability. Apparently, elongation-at-break is fairly decreased due to hindered segmental mobility of PVA polymer chains. Blending AA, constitutes additional hydrogen bonds which perform as reinforcing networks preventing the easy movement of polymer chains. Hence, hydrogen bonding and electrostatic interactions existing among PVA polymeric chains and AA/CA provide good mechanical stability to the membrane structure. The PVA-LY/CA biocomposite membrane displays maximum tensile strength along with good elongation characteristics, which is essentially ascribed to the strong interaction between LY and PVA. These results illuminate the fact that existence of strong electrostatic interaction between PVA and AA, which results in an increase in the rigidity and a reduction in elongation break.

Morphological Studies

The basic morphology of the PVA-AA/CA biocomposite membrane is examined using an SEM and the image is shown in

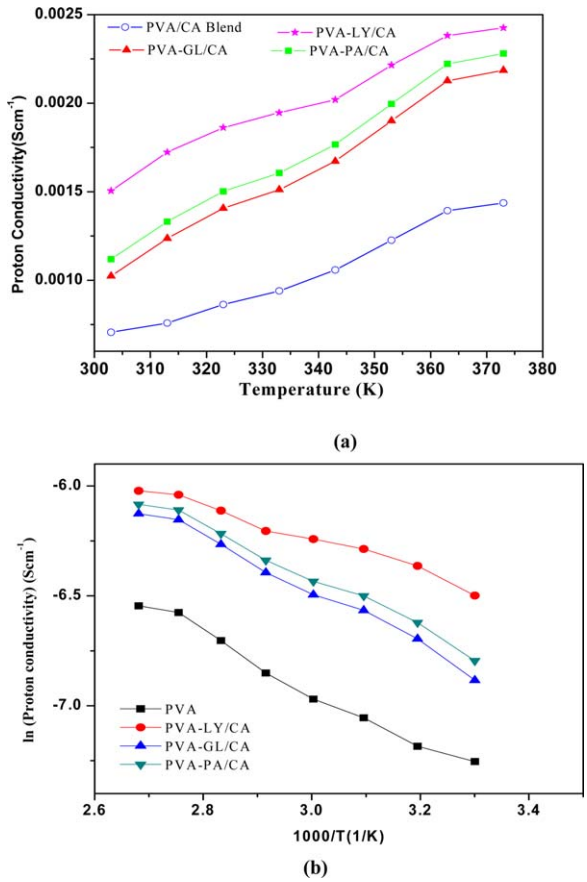

Figure 6. (a) Variation of proton conductivity with temperature for PVA blend, PVA-GL/CA PVA-PA/CA, and PVA-LY/CA biocomposite membranes. (b) ln σ versus 1000/T plot for PVA blend, PVA-GL/CA, PVA-PA/CA, and PVA-LY/CA biocomposite membranes. [Color figure can be viewed in the online issue, which is available at wileyonlinelibrary.com.]

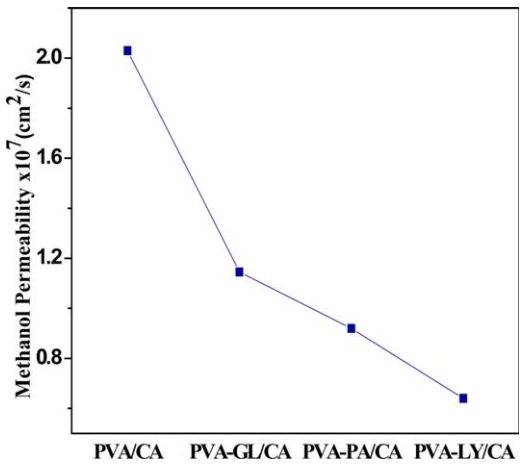

Figure 7. Methanol permeability for PVA blend, PVA-GL/CA, PVA-PA/CA, and PVA-LY/CA biocomposite membranes with methanol concentration 2*M*. [Color figure can be viewed in the online issue, which is available at wileyonlinelibrary.com.]

Figure 5. It is clearly seen from this figure that the PVA-LY/CA biocomposite membrane possess homogeneous, defect-free morphology with no phase separation, implying that the AAs uniformly blended with PVA through favorable electrostatic and hydrogen bonding interactions.

Proton Conductivity and Electrochemical Selectivity of Membranes

Conductivity measurement is significant to assess the ability of a membrane to transfer proton through itself. Figure 6 shows the proton conductivities of PVA blend and PVA-AA/CA biocomposite membranes measured at different temperatures from 303 to 373 K. Proton conductivities are in the range of 10^{-3} to 10^{-2} S/cm. The proton conductivities of all the membranes increased with temperature. Apparently, the proton conductivities of the PVA-AA/CA biocomposite membranes are higher compared to that of PVA blend membrane. AA promotes the proton conduction both through hopping and vehicular mechanisms and dipolar zwitterions rapidly transmit the protons.[43,44] AA constitutes an array of acid–base pairs that acts simultaneously as a proton donor and proton acceptor leads to fast proton transfer through hopping mechanism. Protons interact with carboxylic acid groups and amino groups, transfer via hydrogen bonds formed by PVA with AA and CA. It is noteworthy that functional groups present in CA also involve in hydrogen bonding, thereby increasing the density of hydrogen bonds. These hydrogen bonds offer a path for proton transfer from a proton-donor to a proton-acceptor, which is explained as a fundamental property of hydrogen bonds.[45–48] Vehicular transport of protons is also facilitated by AAs, as they form loose complexes bridged by water molecules. The water molecules entrapped by the basic amino group and acidic carboxylic acid group through the hydrogen bonds transfer the hydrated protons along these bridges. The proton diffuses together with a vehicle (e.g., as H_3O^+) where the counter diffusion of unprotonated vehicles (H_2O) allows the net transport of protons. Accordingly, both Grothuss and vehicular mechanisms are being operated in the PVA-AA/CA biocomposites which results in enhanced proton conductivity. Sorption characteristics have a profound influence on membrane conductivity as higher water sorption facilitates proton transport through the membrane leading to faster proton conduction. It could be inferred that higher proton conductivity observed for PVA-AA/CA biocomposite membranes is mainly due to interplay between zwitterions and PVA. Among all biocomposite membranes, PVA-LY/CA exhibited higher proton conductivity, which is three times more that of PVA blend membrane. Differences in ionic conductivities of biocomposite membranes could be possibly due to the diverse chemical compositions of AAs. Although all AAs studied here have a similar zwitterionic structure, an additional basic amino is present in

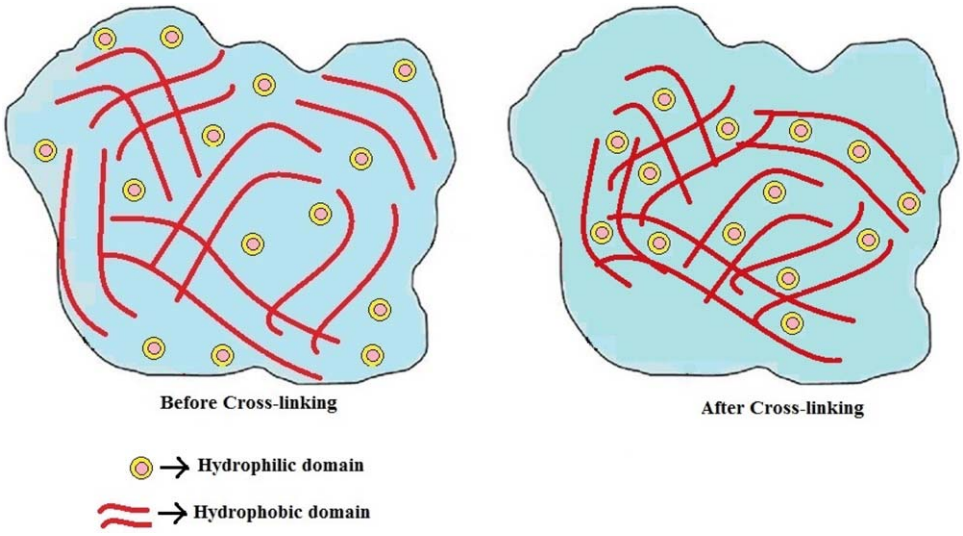

Scheme 2. Schematics illustrating change in hydrophilic/hydrophobic domain structure due to CA crosslinking. [Color figure can be viewed in the online issue, which is available at wileyonlinelibrary.com.]

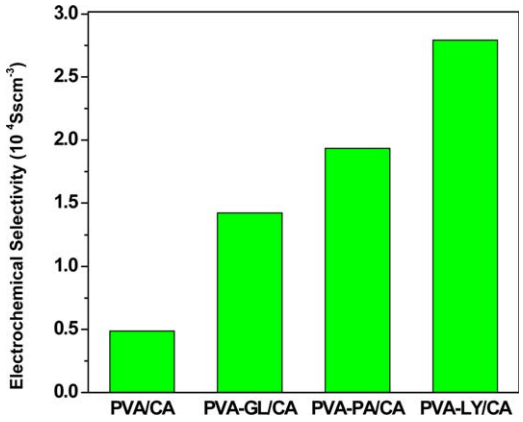

Figure 8. Electrochemical selectivity for PVA blend, PVA-GL/CA, PVA-PA/CA, and PVA-LY/CA biocomposite membranes. [Color figure can be viewed in the online issue, which is available at wileyonlinelibrary.com.]

LY. Comprising two positively charged amino groups, LY actively involved in the interfacial bonding as well as in proton conduction compared to GL and PA with single amino group (amino). An additional amino in LY is responsible for increased ionic conductivity that takes full advantage of PVA polymeric voids to efficiently transmit the protons.

Arrhenius-type temperature dependence of proton conductivity is observed for all membranes studied. Plotting ln σ versus $1/T$, Arrhenius plots were obtained according to eq. (6) given below

$$\sigma = \sigma_0 e^{-}(E_a/RT) \quad (6)$$

In eq. (6), σ is the proton conductivity (S/cm), σ_0 is the pre-exponential factor, E_a is the activation energy (kJ/mol), R is the universal gas constant (8.314 J/mol K), and T is the absolute temperature (K). The E_a values observed for the biocomposite membranes are lower than that of PVA/CA blend membrane, which suggests that the energy required to cross the barrier decreased. Protons are allowed to readily transport over the Eyring's energy barrier through the biocomposite membrane. Similar results were observed for different hydrophilic membranes studied in the literature.[49,50] From the data, E_a value for PVA/CA blend membrane is found to be 29.2 kJ/mol, whereas the E_a values for PVA-GL/CA, PVA-PA/CA, and PVA-LY/CA biocomposites are found to be 25.5, 24.4, and 22.9 kJ/mol, respectively. It is observable from these values that E_a for proton conduction decreases with the incorporation of AA in the PVA matrix. E_a associated with PVA-LY/CA biocomposite membrane is much lower than the other membranes facilitating higher proton conductivity in the former.

Figure 7 shows the methanol permeability data for PVA/CA blend and PVA-AA/CA biocomposite membranes. From the data it could be deduced that methanol permeability through the biocomposite membranes rapidly decreased by an order of magnitude due to presence of AA. In this respect, the changes in the methanol permeability of the membranes could be attributed to many factors, including the changes in the water uptake of the membranes and alteration in a balance between hydrophobic-hydrophilic domain microstructures introduced by CA crosslinking. Schematics of change in hydrophilic/hydrophobic domain structure resulting in methanol mitigating polymeric network is illustrated in Scheme 2. The change in the methanol permeability in the membrane is in good agreement with the sorption results. Accordingly, higher hydrophilic nature of PVA-AA/CA biocomposite membranes favors the selective sorption of water from methanol-water mixture.[47] Hence, due to the change in the microstates, methanol conducting path has been turned into a tortuous one instead of direct pathway. As a result, methanol permeability in the membrane decreased. The methanol crossover rate also differs with the nature of AA. PVA-LY/CA biocomposite membrane has lesser methanol crossover rate compared to both GL and LY containing biocomposites. This could be explained on the basis of higher hydrophilicity of PVA-LY/CA biocomposite membranes and improved interaction between PVA and LY which together leads to closely packed polymeric network thus restricting the methanol flow. The basic nature of LY is the possible reason for the observed results.

For a potential DMFC electrolyte, the membrane should possess both proton conductivity and methanol-barrier property. Since methanol is being permeated through the same channels along which proton conduction also happens, there exists a trade-off between proton conduction and methanol permeability. Electrochemical selectivity of membranes for protons over methanol can be defined as the proton conductivity [σ divided by the methanol permeability (P)], which is often used to evaluate the membrane-electrolyte performance in DMFC. Electrochemical selectivity for PVA/CA blend membrane and PVA-AA/CA biocomposite membranes are presented in Figure 8. Ratio of proton conductivity and methanol permeability should be balanced to improve electrochemical selectivity of the membrane in DMFCs. It is apparent that due to the increase in proton conductivity and decrease methanol crossover flux, selectivity of PVA-AA/CA biocomposites is improved due to presence of AA, designating the augmented comprehensive performance. As expected, selectivity is high for PVA-LY/CA compared to PVA/CA blend and other PVA-AA/CA biocomposites. The reason for the difference in behavior could be related to the structure of the AAs, AA-hydration, and proton conduction through these. The advantage of PVA-LY/CA suggests that both two positively charged amino groups and carboxylic group of LY are engaged in interfacial bonding.[10] These results propose that PVA-LY/CA biocomposite membrane could serve as a good methanol impermeable membrane electrolyte hence and appropriate for DMFC applications.

CONCLUSIONS

The incorporation of the AA biomolecules into PVA, strongly influences the physicochemical properties of the polymer, favors proton conduction, and resists methanol permeation. AA constitutes an array of acid–base pairs that acts simultaneously as a proton donor and proton acceptor leads to fast proton transfer through hopping and vehicular mechanisms. Tuning the conductivity and methanol permeability characteristics of PVA with the assistance of biomolecules is advantageous to promote the

electrochemical selectivity. Biocomposite membranes with well-controlled architecture promote conduction properties simultaneously limits methanol permeation, which is demonstrated by our earlier studies using plant hormones.[51] In addition to this, crosslinking PVA-AA biocomposite with CA substantially improves the membrane properties through balancing hydrophobic-hydrophilic microstates. PVA-AA/CA biocomposite is first of its kind to be utilized as an electrolyte for DMFC. Experimental studies characterizing PVA-AA/CA biocomposites have demonstrated the role of AA and highlighted the possible significance of zwitterions towards selective water sorption characteristics. The rational design of membrane microstructure with proper arrangement of hydrophobic/hydrophilic domains is a key to enhance electrochemical selectivity of PVA-AAs/CA biocomposites.

ACKNOWLEDGMENTS

The author gratefully acknowledges DSKPDF cell (Pune), UGC New Delhi, for the award UGC-D.S. Kothari Post-Doctoral Fellowship. One of the authors S. Mohanapriya is grateful to University Grants Commision (UGC), Government of India, for providing fund under the scheme of 'UGC-Dr. D. S. Kothari Post Doctoral Fellowship'. (Ref: No. Award Letter-No.F.4-2/2006 (BSR)/CH/14-15/0102 dated 5-5-2015).

REFERENCES

1. Antolini, E.; Salgado, J. R. C.; Gonzalez, E. R. *Appl. Catal. B: Environ.* **2006**, *63*, 137.
2. Deluca, N. W.; Elabd, Y. A. J. *Polym. Sci. Part B: Polym. Phys.* **2006**, *44*, 2201.
3. Neburchilov, V.; Martin, J.; Wang, H.; Zhang, J. *J. Power Sources* **2007**, *169*, 221.
4. Scott, K.; Shukla, A. K.; White, R. E.; Vayenas, C. G.; Gamboa-Aldeco, M. A. Modern Aspects of Electrochemistry; Springer: New York, **2006**; Vol. *40*, 127.
5. Mohanapriya, S.; Bhat, S. D.; Sahu, A. K.; Pitchumani, S.; Sridhar, P.; Shukla, A. K. *Energy Environ. Sci.* **2009**, *2*, 1210.
6. Silva, V. S.; Weisshaar, S.; Reissner, R.; Ruffmann, B.; Vetter, S.; Mendes, A.; Madeira, L. M.; Nunes, S. *J. Power Sources* **2005**, *145*, 485.
7. Beatie, P. D.; Orfino, F. P. F.; Basura, V. I.; Zychowska, K.; Ding, J.; Chuy, C.; Scmeisser, J.; Holdcroft, S. *J. Electroanal. Chem.* **2001**, *503*, 45.
8. Fang, J.; Shen, P. K.; Liu, Q. L. *J. Membr. Sci.* **2007**, *293*, 94.
9. Ramya, K.; Dhaththreyan, K. S. *J. Electroanal. Chem.* **2003**, *542*, 109.
10. Kim, D. S.; Park, H. B.; Rhim, J. W.; Lee, Y. M. *J. Membr. Sci.* **2004**, *240*, 37.
11. Antonucci, P. L.; Arico, A. S.; Creti, P.; Ramunni, E.; Antonucci, V. *Solid State Ionics* **1999**, *125*, 431.
12. Ling, J.; Savadogo, O. *J. Electrochem. Soc.* **2004**, *151*, 1604.
13. Othman, M. H. D.; Ismail, A. F.; Mustafa, A. *Malaysian Polym. J.* **2010**, *5*, 1.
14. Jiang, R. Z.; Chu, D. *Electrochem. Solid-State Lett.* **2002**, *5*, A156.
15. Ravikumar, M. K.; Shukla, A. K. *J. Electrochem. Soc.* **1996**, *143*, 2601.
16. Zhang, H.; Li, X.; Zhao, C.; Fu, T.; Shi, Y.; Na, H. *J. Membr. Sci.* **2008**, *308*, 66.
17. Sahu, A. K.; Selvarani, G.; Bhat, S. D.; Pitchumani, S.; Sridhar, P.; Shukla, A. K.; Narayan, N.; Banarjee, A.; Chandrakumar, N. *J. Membr. Sci.* **2008**, *319*, 298.
18. Bhat, S. D.; Aminabhavi, T. M. *J. Membr. Sci.* **2007**, *306*, 173.
19. Smitha, B.; Sridhar, S.; Khan, A. A. *J. Membr. Sci.* **2005**, *259*, 10.
20. Qiu, Y. R.; Zhang, Q. X. *J. Cent. South Uni. Technol.* **2003**, *10*, 117.
21. Li, L.; Xu, L.; Wang, Y. *Mater. Lett.* **2003**, *57*, 1406.
22. Yang, T. *Int. J. Hydrogen Energy* **2008**, *33*, 6772.
23. Tung, C. C.; Lee, Y. J.; Young, J. M. *J. Power Sources* **2009**, *188*, 30.
24. Mohanapriya, S.; Bhat, S. D.; Sahu, A. K.; Manokaran, A.; Vijayakumar, R.; Pitchumani, S.; Sridhar, P.; Shukla, A. K. *Energy Environ. Sci.* **2010**, *3*, 1746.
25. Biggers, J. D.; Summers, M. C.; McGinnis, L. K. *Hum. Reprod. Update* **1997**, *3*, 125.
26. Yesiloglu, Y.; Kilic, I. *Prep. Biochem. Biotechnol.* **2004**, *34*, 365.
27. Chanthad, C.; Wootthikanokkhan, J. *J. Appl. Polym. Sci.* **2006**, *101*, 1931.
28. Kalyani, S.; Smitha, B.; Sridhar, S.; Krishnaiah, A. *Ind. Eng. Chem. Res.* **2006**, *45*, 9088.
29. Lin, C. W.; Huang, Y. F.; Kannan, A. M. *J. Power Sources* **2007**, *171*, 340.
30. Tsai, C. E.; Lin, C. W.; Hwang, B. J. *J. Power Sources* **2010**, *195*, 2166.
31. Bolto, B.; Tran, T.; Hoang, M. *Prog. Polym. Sci.* **2009**, *34*, 969.
32. Aparicio, M.; Castro, Y.; Duran, A. *Solid State Ionics* **2005**, *176*, 333.
33. Reddy, N.; Yang, Y. G. *Food Chem.* **2010**, *118*, 702.
34. Park, H. R.; Chough, S. H.; Yun, Y. H.; Yoon, S. D. *J. Polym. Environ.* **2005**, *13*, 4.
35. Li, L.; Wang, Y. *J. Membr. Sci.* **2005**, *262*, 1.
36. Soled, S.; Misceo, G.; McVicker, W. E.; Gates, A.; Guiterrez, A.; Paes, J. *Catal. Today* **1997**, *36*, 441.
37. Kang, S.; Lee, S. J.; Chang, H. *J. Electrochem. Soc.* **2007**, *154*, B1179.
38. Chen, Y. C.; Jer, C. S.; Tong, L. K.; Chen, C. W.; Tseng, L. C.; An, H. C. *J. Power Sources* **2008**, *184*, 44.
39. Song, K. Y.; Lee, H. K.; Kim, H. T. *Electrochim. Acta* **2007**, *53*, 637.
40. Perry, R. H.; Green, D. W.; Maloney, J. D. In Perry's Chemical Engineers Hand Book, 7th ed.; McGraw-Hill, **1997**.
41. Jiang, R.; Chu, D. *J. Electrochem. Soc.* **2004**, *151*, A69.
42. Mohanapriya, S.; Bhat, S. D.; Sahu, A. K.; Manokaran, A.; Pitchumani, S.; Sridhar, P.; Shukla, A. K. *J. Bionanosci.* **2009**, *3*, 131.
43. Ogawa, T.; Aonuma, T.; Tamaki, T.; Ohashi, H.; Ushiyama, H.; Yamashaita, K.; Yamaguchi, T. *Chem. Sci.* **2014**, *5*, 4878.

44. Yin, Y.; Xu, T.; He, G. N.; Jiang, Z.; Wu, H. *J. Power Sources* **2015**, *276*, 271.
45. Paddison, S. *J. Annu. Rev. Mater. Res.* **2003**, *33*, 289.
46. Crank, J. The Mathematics of Diffusion; Clarendon Press: Oxford, UK, **1975**.
47. Kreuer, K. D. *Solid State Ionics* **2000**, *136*, 149.
48. Kreuer, K. D. *Chem. Mater.* **1996**, *8*, 610.
49. Li, L.; Zhang, J.; Wang, Y. *J. Membr. Sci.* **2003**, *226*, 159.
50. Smitha, B.; Sridhar, S.; Khan, A. A. *J. Power Sources* **2006**, *159*, 846.
51. Mohanapriya, S.; Sahu, A. K.; Bhat, S. D.; Pitchumani, S.; Sridhar, P.; George, C.; Chandrakumar, N.; Shukla, A. K. *J. Electrochem. Soc.* **2011**, *158*, A1.